A Time Domain Beamforming Algorithm for SAR Tomography

Matteo Nannini, Rolf Scheiber
German Aerospace Center (DLR), Microwaves and Radar Institute (HR), Oberpfaffenhofen, Germany.
e-mail: *matteo.nannini@dlr.de*

Abstract

Interest on 3D imaging in a remote sensing frame has grown in the recent years and it finds in SAR Tomography (TomSAR) a natural way to resolve for targets in the third dimension. In this paper we compare the performance of a pure beamforming technique with the SpecAn algorithm. This comparison has the goal to estabilish if the time domain beamforming (TDB) performance are efficient in order to perform tomographic focusing. A tomographic baseline calibration is also presented. The TDB is applied on simulated and real airborne data in L-band. The real data have been acquired during a tomographic campaign in May 1998 on the test site of Oberpfaffenhofen (Germany) with the E-SAR system of the German Aerospace Center (DLR).

1 Introduction

SAR Interferometry (InSAR) is a first step toward 3D imaging, but it allows only to recover information related to the mean phase center of all the targets present in a resolution cell. Polarimetric SAR interferometry (PolInSAR) allows a phase center separation between targets within a resolution cell if their polarimetric behaviour is different, but it fails to resolve them when they answer with the same scattering mechanism.
The basic idea behind TomSAR is to resolve for targets with different heights inside a resolution cell by building an aperture in the zero Doppler plane (direction perpendicular to the synthetic aperture). Extending SAR analysis in this way, it is possible to focus the 3D target (see fig.1).

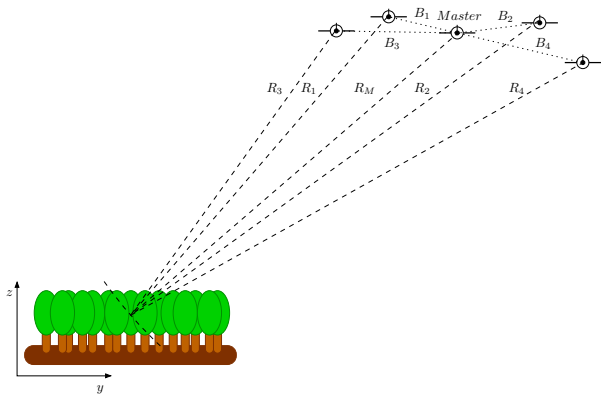

Figure 1: Airborne tomographic acquisition geometry.

It has to be pointed out that the targets of interest are mostly volume-distributed, therefore their model as point-like does not fit completely with the reality [1] and that tomography is actually a 3D problem that should be faced in all the three dimensions at the same time but, if the aperture dimension is smaller compared to the slant-range distance then it is possible to separate the focusing in three steps (range-azimuth-tomographic direction). In fact in [2] it is shown that an extension of SAR focusing can succesfully face tomographic problems and provide reliable results.
The so called *SpecAn* algorithm which exploits some analogy between the TomSAR and ScanSAR signal, was used for the first demostration on real airborne data.
Within this paper we want to overcome some drawbacks of this algorithm and check how the TDB [3] could efficiently perform 3D focusing.
The resolution ρ_h of the focused image depends on the length L of the tomographic aperture:

$$\rho_h = \frac{\lambda R_M}{2 L}. \tag{1}$$

If R_M is around $5000m$, L must be not less then $300m$, to achieve a resolution of about $2m$. Fixed L also an acquisition geometry has to be pointed out in a way that the distance d between two tracks will undergo the Nyquist theorem. In this way a lower bound on the number of tracks has to be introduced. The volume that will be possible to focus without aliasing will have a height:

$$h_0 \leq \frac{\lambda R_{Master}}{2 d}. \tag{2}$$

At the same time an upper bound on the maximum number of observations has to be defined due to feasibility constraints. Another important effect to take into account is that each track is independent from the other, hence strong irregular sampling along the tomographic aperture is present [2], common to airborne and spaceborne case.

2 Time Domain Beamforming

The SAR tomography acquisition geometry is depicted in fig.1, where as example 5 sensors are looking the same scene and are separated from the master by a baseline B_i. It is easy to understand the analogy between this geometry and the azimuth one of a SAR survey, but despite their similarity their related received signals have different characteristics.
With the set of n coregistered SAR images $[s_1, s_2, \cdots, s_n]$ a tomographic signal $s_t(r, a)$ for each range-azimuth coordinates (r, a) can be defined as:

$$s_t(r, a) = [s_1(r, a), s_2(r, a), \cdots, s_n(r, a)]\,. \qquad (3)$$

For the following analysis we will refere to $s_t(i)$ as a componet of the tomographic signal related to the i^{th} SAR image at the coordinate (r_0, a_0).
The SpecAn approach consists basically in two steps: the first is a quadratic phase compensation called *deramping* and the second is a Fourier transform [2].
Once that a reference point at a height h_{ref} has been chosen, a deramping function is defined. If now a target moves away from h_{ref} the deramping function will not perfectly match the tomographic signal $s_t(i)$ and a defocusing will occur.
To prove that, the SpecAn algorithm has been applied on a simulated data set consisting of two point targets located at heights $h_{ref} = 0m$ and $h_1 = 7.5m$ viewed by 15 equally spaced sensors located at a height of $3200m$ with a resulting tomographic aperture of $300m$.

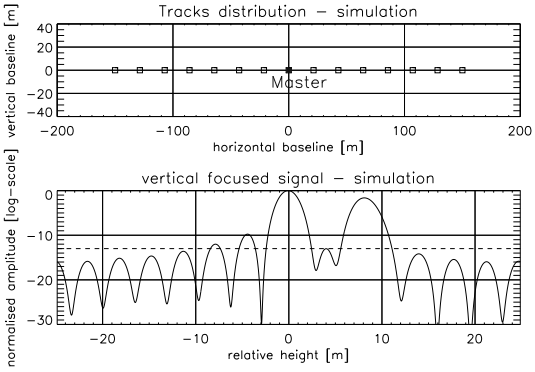

Figure 2: SpecAn results for two point targets and a regular sampled acquisition geometry.

The result is summarized in fig.2 where it is possible to observe that the target at a height h_1 is defocused and also its related amplitude is less than the reference one.
In addition, in a real tomographic airborne acquisition (section 3) the tracks are irregularly spaced and this will result in an unevenly sampled signal. A Fourier based technique like SpecAn is very sensible to the uneven nature of the acquisition and, therefore, the algorithm performance drastically change when such a situation is present.

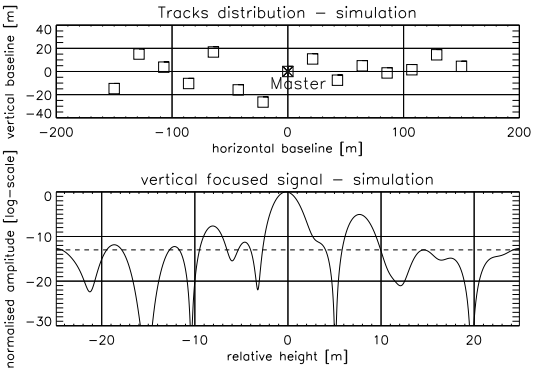

Figure 3: SpecAn results for two point targets and an irregularly spaced acquisition geometry.

Fig.3 represents the focused signal related with the two points of the previous example with irregular acquisition (in the upper part of the figure is depicted the acquisition geometry). With such a situation the target at height h_1 is not focused at all.
To overcome this drawback a resampling to regular grid is needed, but a simple interpolation is not applicable due to the long distance in term of wavelength between the tracks (20m in average). This is why in [2] a generation of synthetic tracks before the regularisation was also required. These SpecAn drawbacks lead us to compare it with a pure TDB technique in which every element inside the volume is focused with an *ad hoc* reference function resulting in a perfect target detection. These set of reference functions can be written as:

$$ref_h(i) = e^{j\frac{4\pi R_i^h}{\lambda}} \qquad 0 \le i \le n-1 \qquad (4)$$

where R_i^h is the generic distance i^{th} track - target located at a height h. The element of the focused signal related to the height h will be:

$$s_f(h) = \sum_{i=0}^{n-1} s_t(i)\, ref_h(i) \qquad (5)$$

and now varying h between h_{min} and h_{max} the resulting focused signal will be represented by:

$$out = [s_f(h_{min}), \cdots, s_f(h), \cdots, s_f(h_{max})]\,. \qquad (6)$$

With TDB no defocusing occurs for both the even and uneven sampling. Therefore it is possible to work directly in the real situation without any resampling or regularisation. Fig.4 presents the result of the TDB algorithm applied on the same irregularly spaced acquisition data set. It is possible to observe how, with the TDB, both targets are correctly focused.

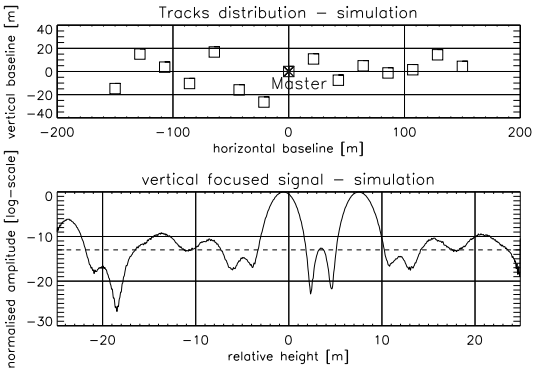

Figure 4: TDB results for two point targets and an irregularly spaced acquisition geometry.

3 Experiment - Results

3.1 Data Set

The TDB has been tested on a set of real data acquired by the E-SAR system of the DLR (German Aerospace Center) in May 1998, during a tomographic campaign. A number of 14 tracks were flown with an averaged baseline of $20m$ building a tomographic aperture of approximated $240m$ with a mean R_M of $4600m$, which allows to focus a volume of $30m$ with a theoretical resolution around $2.5m$. Fig.5 represents the nominal acquisition geometry.

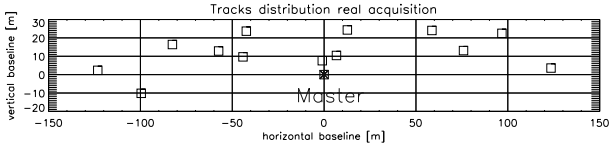

Figure 5: Tomographic campaign acquisition geometry (nominal tracks).

In order to apply the TDB a precise knowledge of the sensors position is needed because from it depends the reliability of the reference functions. In fact variable errors in the order of $10cm$ on the tracks position will not allow a reliable focusing. To avoid this problem modern motion compensation techniques [4] have been applied. After this operation it is possible to assume a straight line as the flight path for the aircraft. At this point the tomographic signal is still not ready to be used to perform 3D focusing, because of unknown offsets in the absolute baselines (due to the limits in the absolute navigation system accuracy) that need to be compensated. To do that a baseline calibration step is required (section 3.2) after which the TDB can be applied.

3.2 Tomographic Baseline Calibration

Let us consider a corner reflector (CR) located at a known height and at the coordinates (r_{CR}, a_{CR}) in the SLC image. Defining $\phi_{M,i}$ the interferometric phase $Master - i^{th}$ track in (r_{CR}, a_{CR}) and $\phi_{M,i}^{geom}$ as the phase difference computed with the tracks and the CR position, the expected difference $\phi_{M,i} - \phi_{M,i}^{geom}$ should be equal to zero, but due to the residual navigation system errors a phase offset is present. In order to perform the tomographic focusing this offset need to be compensated independently in every pair of images. Under the hypothesis that the aircrafts are flying on a straight line, the baseline errors E_{B_y}, E_{B_z} in the vertical and horizontal directions, can be estimated by a functional minimisation.
For each CR is possible to write that:

$$\phi_{M,i}^{geom}(E_{B_y}, E_{B_z}) = -\frac{4\pi}{\lambda}(\sqrt{y_M^2 + z_M^2} - \sqrt{(y_M + B_y + E_{B_y})^2 + (z_M + B_z + E_{B_z})^2}\ ) \quad (7)$$

where y_M and z_M are respectively the horizontal and the vertical distance $Master - CR$ and B_y and B_z are the vertical and horizontal baseline. Now, exploiting the fact that in our scene eight CRs are present, the following functional can be defined:

$$G(E_{B_y}, E_{B_z}) = \sqrt{\sum_{k=1}^{8} (\phi_k^{geom}(E_{B_y}, E_{B_z}) - \phi_k)^2} \quad (8)$$

where ϕ_k is the unwrapped interferometric phase upon the known height of the k^{th} CR (for the sake of simplicity the indexes M, i are omitted in the phase expressions). The minimisation results consists in the estimation of the baseline errors with which B_y and B_z can be updated. Table 3.2 shows the absolute correction values. It is interesting to observe that the standard deviation is around $10cm$ in perfect agreement with the assumed navigation system precision.

Related Track	Baseline error [cm]	Baseline [m]
1	16,11	7.64
2	6,52	12.41
3	7,87	45.20
4	11,67	27.41
5	14,11	48.51
6	17,71	63.42
7	5,07	58.84
8	20,74	77.00
9	7,41	84.19
10	6,50	99.36
11	8,45	100.09
12	3,58	123.57
13	10,24	123.24

Table 1: Baseline calibration results: track, absolute baseline error, baseline.

3.3 Results

In fig.6 a the tomographic signal $s_t(r_{CR}, a_{CR}, i)$ related to a CR has been focused with the TDB approach.

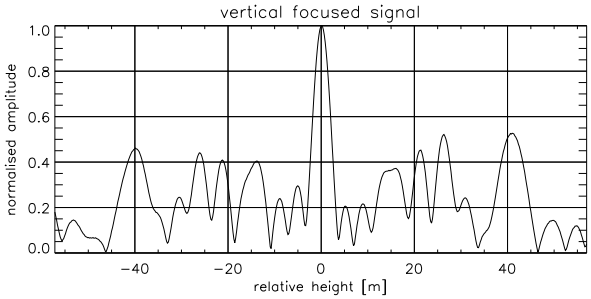

(a)

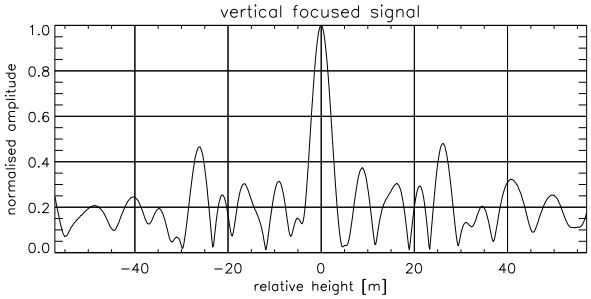

(b)

Figure 6: TDB with a single CR as a calibration reference (a) and with all the CRs and the implemented calibration method (b).

The figure shows a comparison between the results of a phase calibration made with only one CR and the applied technique. It is possible to see how the CR response has been depured from undesired components, resulting in lower sidelobs. The focused pulse in fig.6(b) shows the main limitation in the use of a pure TDB: the presence of ambiguities at the height $h_a = \frac{\lambda R_{Master}}{2\,d} \cong 27m$. As said standard interpolation methods to reduce ambiguities can not be used in the TomSAR context. In fig.7 the focused tomographic signal produced by interpolated TDB based on the tracks regularisation described in [2] is presented. Due to the more dense sample frequency (increased by a factor of 10) the ambiguities do not appear at all. This regularisation is valid only under the assumption that a main scatterer is present in the scene. When this is not the case (volume-distributed targets) the focusing performance of the algorithm does not improve.

4 Conclusion

In this paper we present the comparison between the SpecAn and the TDB algorithm in order to perform tomographic focusing. In an irregularly distributed acquisition geometry the TDB algorithm can focus point targets located at different heights without any loss in detection and resolution with respect to the SpecAn algorithm. The algorithm shows its limitation due to the sensitivity to height ambiguities that could possibly be overcomed with more robust beamforming techniques [5]. The paper describes also a tomographic baseline calibration in order to compensate the phase offsets among all the 2D images.

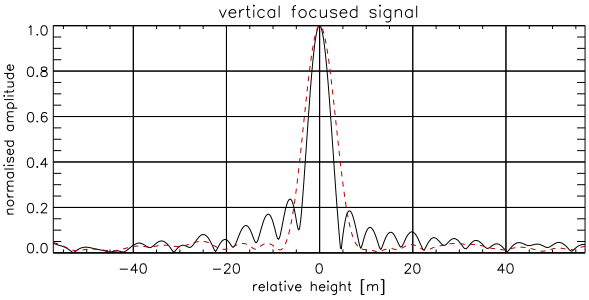

Figure 7: Interpolated TDB by means of synthetic tracks generation. Without Hamming window (solid black line) and with Hamming window (dashed red line).

References

[1] F. Lombardini et al.: *Reflectivity estimation for multibaseline interferometric radar imaging of layover extended sources*, Signal Processing, IEEE Transactions on Volume 51, Issue 6, June 2003.

[2] A. Reigber, A. Moreira: *First demonstration of airborne SAR tomography using multibaseline L-band data*, Geoscience and Remote Sensing, IEEE Transactions on Volume 38, Issue 5, Part 1, Sept. 2000 Page(s):2142 - 2152.

[3] J. Homer et al.: *High resolution 3D SAR via multibaseline interferometry*, Geoscience and Remote Sensing Symposium, 1996. IGARSS '96. Volume 1, 27-31 May 1996 Page(s):796 - 798 vol.1.

[4] P. Prats et al.: *Interpolation-free coregistration and phase-correction of airborne SAR interferograms*, Geoscience and Remote Sensing Letters, IEEE Volume 1, Issue 3, July 2004 Page(s):188 - 191.

[5] F. Lombardini et al.: *Adaptative spectral estimation for multibaseline SAR Tomography with airborne L-band data*, Geoscience and Remote Sensing Symposium, 2003. IGARSS '03. Proceedings. 2003 IEEE International Volume 3, 21-25 July 2003 Page(s):2014 - 201.6